Molecular and Thermal Diffusion Coefficients of Alkane−Alkane and Alkane−Aromatic Binary Mixtures: Effect of Shape and Size of Molecules

Alana Leahy-Dios and Abbas Firoozabadi*

Department of Chemical Engineering, Mason Lab, Yale University, New Haven, Connecticut 06520-8286

Received: July 24, 2006; In Final Form: October 27, 2006

New molecular and thermal diffusion coefficients of binary mixtures of normal decane−normal alkanes and methylnaphthalene−normal alkanes are measured at atmospheric pressure and $T = 25$ °C. The normal alkanes used in this work include nC_5−nC_{20}. Thermal diffusion coefficients were measured in a thermogravitational column. Molecular diffusion coefficients were measured using an open-ended capillary tube technique. Results show a significant effect of molecular shape and size on thermal and molecular diffusion coefficients. Molecular diffusion coefficients show a monotonic behavior in both aromatic−normal alkane and normal decane−normal alkane mixtures. Thermal diffusion coefficients reveal a nonmonotonic trend with molecular size in the normal decane−normal alkane mixtures. This is the first report of the nonmonotonic behavior in the literature. The data presented in this paper provide an accurate self-molecular diffusion coefficient for nC_{10} from binary data.

I. Introduction

Molecular and thermal diffusion processes with a myriad of applications[1] are quantified by molecular and thermal diffusion coefficients, D and D^T, respectively. These coefficients are generally functions of temperature T, pressure P, and composition ω of the mixture. However, the dependency of D and D^T on T, P, and ω has not been fully understood and determined either theoretically or experimentally. Mass-based molecular and thermal diffusion coefficients in a binary mixture relate to mass diffusion flux of component 1 according to

$$J_1 = -\rho(D\nabla\omega_1 + \omega_1(1 - \omega_1)D^T\nabla T) \quad (1)$$

where ρ is the mixture mass density, $\nabla\omega_1$ is the mass fraction gradient of component 1, and ∇T is the temperature gradient. In eq 1, the entire term $\omega_1(1 - \omega_1)D^T$ is often referred to as the thermal diffusion coefficient. Note that based on thermodynamic stability analysis, when the thermal diffusion coefficient is positive, the component should segregate to the cold side in a binary mixture;[2] there is no need to adopt a sign convention.

This work centers on binary molecular and thermal diffusion coefficients in hydrocarbon liquid mixtures. We are interested in (1) studying the D and D^T dependency on alkane chain size by measuring both diffusion coefficients for a set of binary mixtures of 1-methylnaphthalene (an aromatic) and various normal alkanes and for a second set of normal decane and various other normal alkanes and (2) investigating molecular shape effects on molecular and thermal diffusion coefficient by comparing both sets. The aromatic 1-methylnaphthalene and normal decane have nearly the same molecular weight but very different molecular shapes; by comparing results for these two sets one may obtain a better understanding of the effect of molecular shape on D and D^T for this set of hydrocarbon mixtures. According to Kempers,[3] energetic interactions (chemical contributions), followed by size or shape of molecules, are important parameters in thermal diffusion in liquids. We believe that the size and shape of molecules are closely related to the way they interact with each other. The types of bonds and atoms present in a molecule define its shape, chemical activity, and energetic interaction with other molecules.

In the past, Hayduck and Buckley[4] investigated the effect of molecular shape and size on D for mixtures of normal alkanes at infinite dilution in normal hexane and carbon tetrachloride; they found that D for the essentially linear mixtures were generally 30% higher than D for essentially spherical mixtures. Measurements have been conducted to study compositional effects for D of alkane−alkane,[5] alkane−carbon tetrachloride,[6] and alkane−chloroform[7] binary mixtures over a limited alkane range and for D^T of heptane−hexadecane mixtures.[8] Experimental studies on the effect of isotope substitution on D^T and D have been conducted for binary mixtures of benzene, cyclohexane, and hexane.[9,10] Measurements for D^T have been performed for some alkane−alkane mixtures (pentane−decane[11] and alkane (nC_5−nC_{13})−octadecane[12]) and monocyclic aromatic−alkanes mixtures—benzene[13−15] and toluene[15,16] with alkanes (nC_7−nC_{15}). Measurements are much more limited for polycyclic aromatic−alkane mixtures.[3,17,18] The data presented in this work covers a wider range of alkane molecular weights than the data in refs 3−18.

This paper is organized as follows: In section II we present mixtures and equipment used and explain the composition analysis performed. Next, we describe the thermogravitational technique used for measuring thermal diffusion coefficients (section III) and the open-ended capillary tube technique used for determining molecular diffusion coefficients (section IV). We present the results in section V and provide a discussion in section VI. Finally, we conclude the work in section VII.

II. Experimental Methods

A. Setup Validation. We recently designed and constructed the experimental setups to conduct the measurements in this work. Before embarking on new measurements, we validated

* To whom correspondence should be addressed. E-mail: abbas.firoozabadi@yale.edu.

10.1021/jp064719q CCC: $37.00
Published on Web 12/14/2006

TABLE 1: Density (ρ), Compositional Coefficient (γ), Thermal Expansion Coefficient (α), and Dynamic Viscosity (μ) for All Mixtures at $T = 25.0$ °C, $P = 1$ atm, and $\omega_1 = 50$ wt %[a]

mixture	ρ (g/cm^3)	γ	α (10^{-4} K^{-1})	μ (10^{-3} Pa·s)
		SET 1: MN−nC$_i$		
MN−nC$_5$	0.781801	0.4974	11.463	0.479
MN−nC$_6$	0.803980	0.4385	10.536	0.606
MN−nC$_7$	0.819834	0.4011	9.931	0.741
MN−nC$_8$	0.832711	0.3745	9.387	0.891
MN−nC$_9$	0.841786	0.3528	9.236	1.076
MN−nC$_{10}$	0.849696	0.3347	9.074	1.244
MN−nC$_{11}$	0.856195	0.3196	8.888	1.464
MN−nC$_{12}$	0.86206	0.3101	8.660	1.683
MN−nC$_{14}$	0.870364	0.2913	8.452	2.135
MN−nC$_{16}$	0.876892	0.2753	8.298	2.649
		SET 2: nC$_{10}$−nC$_i$		
nC$_{10}$−nC$_5$	0.672013	0.1555	12.914	0.405
nC$_{10}$−nC$_6$	0.689862	0.1037	11.998	0.476
nC$_{10}$−nC$_7$	0.702472	0.0662	11.386	0.563
nC$_{10}$−nC$_8$	0.712331	0.0382	10.961	0.653
nC$_{10}$−nC$_{12}$	0.735718	−0.0268	10.059	1.068
nC$_{10}$−nC$_{14}$	0.742671	−0.0414	9.824	1.299
nC$_{10}$−nC$_{16}$	0.747700	−0.0591	9.644	1.557
nC$_{10}$−nC$_{20}$	0.754966	−0.0784	9.385	2.102

[a] Uncertainty of viscosity measurements is less than 1%. Density, γ, and α coefficient accuracies are limited by the densitometer and balance precisions.

the setups and procedures using four binary mixtures: the three binary mixtures composed of pairwise combinations of tetrahydronaphthalene, normal dodecane, and isobutylbenzene at 25.0 °C and 50 wt % of each component and the binary mixture water−ethanol at 25.0 °C and 60.88 wt % water. The first three mixtures have been used in a benchmark test[18] to compare various experimental techniques, and the last mixture has been widely studied in the literature[19−23] at temperatures close to 25 °C.

B. Mixtures Studied. Table 1 shows the binary mixtures of this work along with density, compositional coefficient $\gamma = \rho_0^{-1}(\partial\rho/\partial\omega)$, thermal expansion coefficient, and dynamic viscosity. From here on, 1-methylnaphthalene will be referred to as MN, tetrahydronaphthalene as THN, isobutylbenzene as IBB, water as H_2O, ethanol as EtOH, and normal alkanes as nC$_i$ (i = number of carbon atoms); the set of MN−nC$_i$ binary mixtures will be referred to as SET 1 and the set of nC$_{10}$−nC$_i$ binary mixtures as SET 2. Measurements were performed at 25.0 °C and 1 atm. The composition of all mixtures was 50 wt % of each component, except for the H_2O−EtOH mixture (60.88 wt % H_2O). The heaviest normal alkane in this work is nC$_{20}$. The mixture nC$_{10}$−nC$_{20}$ is liquid at the measuring conditions, while MN−nC$_{20}$ is in a liquid−solid state; for that reason, the last mixture in SET 1 is MN−nC$_{16}$ and in SET 2 nC$_{10}$−nC$_{20}$.

All reagents were purchased from Acros Organics, except for nC$_9$, nC$_{11}$, nC$_{14}$, nC$_{16}$, and nC$_{20}$ (TCI America) and EtOH (Pharmco-AAper). All reagents had a purity of 99% or higher, except for MN (97%), tetrahydronaphthalene, and n-nonane (98%); all fluids were used without further refining.

C. Equipment. The thermogravitational column and open-ended capillary apparatus were constructed in our laboratory and are explained in detail in sections III and IV. Density was measured by the Anton PAAR densimeter DMA 5000 with an estimated temperature fluctuation of ±0.005 °C and accuracy of $\pm 2 \times 10^{-6}$ g/cm^3. The samples were weighted on a digital scale with a precision of ±0.0001 g. Viscosity measurements were performed on a Haake Falling-Ball viscometer with a typical accuracy of greater than 99%. Water bath temperature control had an accuracy of ±0.1 °C.

D. Composition Analysis. The composition of a given mixture (subjected to a temperature or concentration gradient) is needed to determine D and D^T. In our mixtures, we may have very small composition changes and therefore need accurate means of measuring these changes, not attainable by analytical methods such as gas or liquid chromatography. To obtain accurate measurements of the composition of a binary mixture, we measure the density using a very precise densitometer and relate it to its composition via calibration. We do not assume the ideal liquid mixture but that the density of a given binary mixture is a linear function of its composition

$$\rho \approx \rho^0 + \frac{\partial\rho}{\partial\omega_1}(\omega_1 - \omega_1^0) \tag{2}$$

For small composition changes, the derivative $\partial\rho/\partial\omega_1$ is constant and eq 2 can be written as

$$\rho = a_0 + a_1\omega_1 \tag{3}$$

where a_0 and a_1 are constant parameters. To create the calibration curve and determine a_0 and a_1 for each binary mixture, we measure the density of seven mixtures with compositions around that of the mixture of interest and determine a_0 and a_1 by fitting eq 3 to density and composition data. Once a_0 and a_1 are known, we determine the composition of a sample by measuring ρ and calculating ω_1 from eq 3 and ω_2 by mass balance ($\omega_2 = 1 - \omega_1$). Figure 1a shows that density varies linearly in the range of our calibration, and therefore eq 3 applies. Linearity is observed in all other mixtures as well.

III. Thermal Diffusion Coefficient

We use the thermogravitational column technique to determine thermal diffusion coefficients. A schematic of the thermogravitational column is shown in Figure 2. This technique consists of measuring the compositional gradient of a mixture inside a thin column submitted to a linear temperature gradient. Our thermogravitational column comprises of two rectangular hollow aluminum tubes connected to each other on the top and bottom parts by an aluminum spacer, creating a gap between two sides of the tubes. The gap is created by attaching glass plates to the remaining sides of the equipment, so that visual inspection is possible throughout the experiment. The mixtures are charged into the column by two holes in the top spacer. Each side of the column is connected to a circulating water bath at constant but different temperatures, establishing a temperature gradient inside the column. After the column is charged with a mixture and steady state is reached, samples are taken from five equally spaced vertical sampling ports and their concentration determined by density measurement. The average temperature in the column is 25.0 °C. We used a temperature difference across the column of 5 and 10 °C to verify that mixture separation is independent of the imposed temperature gradient. The dimensions of the column are $L_z = 46.7 \pm 0.1$ cm, $L_y = 4.7 \pm 0.1$ cm, and $L_x = 1.60 \pm 0.02$ mm. A critical element of the column is a very uniform thickness L_x along the entire length. We verified gap uniformity by measuring the thickness along the column height using very precise gauges. The precision in L_x is a reflection of gap uniformity.

Furry, Jones and Onsager[24] developed the theory for determining the thermal diffusion coefficients of binary gas mixtures in a thermogravitational column, and Majumdar[25] extended the theory to concentrated solutions. The aspect ratio L_z/L_x of the thermogravitational column is very high, which allows for the following simplifying assumptions: (1) the horizontal velocity

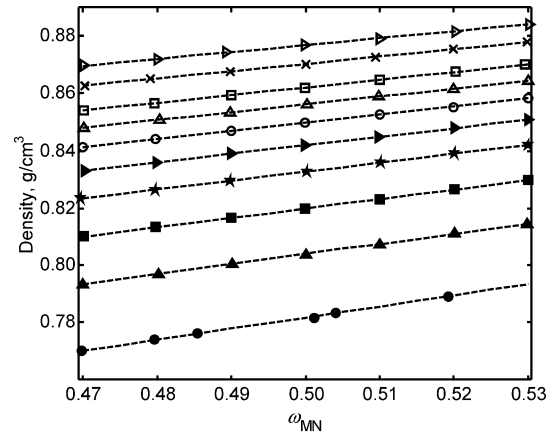

(a)

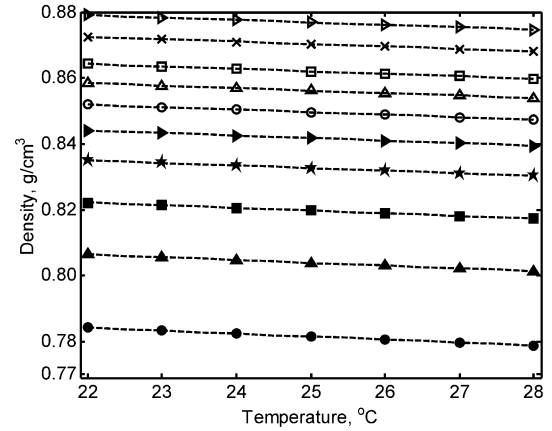

(b)

Figure 1. Density variation with composition (a) and temperature (b) at 25.0 °C and 50 wt % of each component for the binaries MN−nC_5 (●), MN−nC_6 (▲), MN−nC_7 (■), MN−nC_8 (★), MN−nC_9 (solid right-facing triangle), MN−nC_{10} (○), MN−nC_{11} (△), MN−nC_{12} (□), MN−nC_{14} (×), and MN−nC_{16} (open right-facing triangle). The dashed lines represent linear fits to the data.

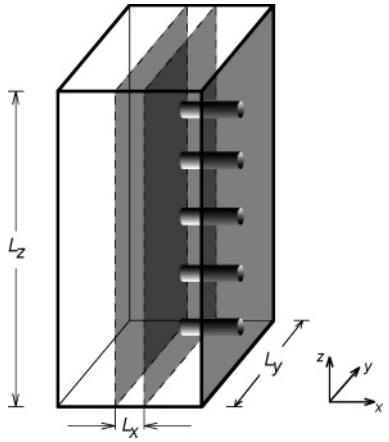

Figure 2. Sketch of the thermogravitational column, not to scale. The five sampling ports are shown, but the inlets/outlets for water circulation on each side of the column are not shown for clarity. Dimensions are given in the text.

component is negligible; (2) there is no vertical temperature gradient; (3) the linear Boussinesq approximation is valid; (4) density is only a function of temperature; and (5) vertical molecular diffusion flux is negligible compared to vertical convection flux. The following equation gives the thermal diffusion coefficients for component 1 in a binary mixture (see Haugen and Firoozabadi[26] for complete development of the working equation)

$$D^{\mathrm{T}} = \frac{\rho_0 g \alpha {L_x}^4}{504 \mu \omega_1 (1-\omega_1)} \frac{\Delta\omega_1}{\Delta z} \tag{4}$$

In eq 4, α is the thermal expansion coefficient $\alpha = -\rho_0^{-1})(\partial\rho/\partial T)$, g the gravitational acceleration, μ the dynamic viscosity, and $(\Delta\omega_1/\Delta z)$ is the composition gradient of component 1 at steady state. Note that the separation in the column is independent of the temperature difference between the cold and hot plates, as stated earlier.

IV. Molecular Diffusion Coefficient

We use the open-ended capillary tube technique[27] for molecular diffusion coefficient measurements. Tubes of length $L = 38.98 \pm 0.08$ mm and volume $V = 1.00$ cm^3 are filled with a binary mixture of known composition $\omega_{1,0}$ and immersed in a bath of much larger volume ($V \approx 450$ cm^3) of the same binary mixture of composition $\omega_{1,\infty}$, kept constant by means of agitation. Temperature is maintained at 25.0 °C by use of double-jacketed beakers connected to a circulating water bath.

The mass balance of the heavier component of a binary mixture in the one-dimensional capillary tube described above is written as

$$\frac{\partial\omega_1}{\partial t} = D\frac{\partial^2\omega_1}{\partial z^2} \tag{5}$$

In eq 5, t is the time and z is the vertical distance (positive downward). Local mass balance requires an extra (convective) term on the right-hand side of eq 5. However, in this case the convective velocity inside the capillary tube is very small and this term is negligible.

The initial and boundary conditions are

$$\omega_1(z,0) = \omega_{1,0},\ \omega_1(0,t) = \omega_{1,\infty},\ \left.\frac{\partial\omega_1}{\partial z}\right|_{z=L} = 0 \tag{6}$$

where $\omega_{1,0}$ is the initial mass fraction of component 1 and $\omega_{1,\infty}$ is the mass fraction of the same component at the tube outlet (the composition in the large bath). Integration of eq 5 and use of the boundary and initial conditions given in eq 6 yield the concentration inside each tube at time t and length z

$$\omega_1 - \omega_{1,\infty} = \frac{4(\omega_{1,0}-\omega_{1,\infty})}{\pi}\sum_{m=0}^{\infty}\frac{\sin\left((m+1/2)\frac{\pi}{L}z\right)\exp\left(-\frac{\pi^2(m+1/2)^2}{L^2}Dt\right)}{(2m+1)} \tag{7}$$

The average mass fraction of component 1 inside the tube at time t is given by

$$\langle\omega_1\rangle - \omega_{1,\infty} = \left[\frac{8(\omega_{1,0}-\omega_{1,\infty})}{\pi^2}\sum_{m=0}^{\infty}\frac{\exp\left(-\frac{\pi^2(m+1/2)^2}{L^2}Dt\right)}{(2m+1)^2}\right] \tag{8}$$

In 12-h intervals, a tube is taken out of the bath and its average composition $\langle\omega_1\rangle$ determined by density measurement. After a

TABLE 2: Compositional Coefficient (γ), Thermal Expansion Coefficient (α), and Dynamic Viscosity (μ) for the Mixtures Used for Validation of Experimental Setup and Procedure in This Work[a]

	γ			α (10^{-4} K^{-1})			μ (10^{-3} Pa·s)		
mixtures	lit.	this work	max Δ	lit.	this work	max Δ	lit.	this work	max Δ
THN−nC_{12}[18]	0.2362	0.2565	8.6%	9.227	8.949	3.0%	1.59	1.51	5.0%
THN−IBB[18]	0.1312	0.1287	1.9%	8.881	8.853	0.3%	1.45	1.38	4.8%
IBB−nC_{12}[18]	0.1306	0.1280	2.0%	9.893	9.623	2.7%	1.1	1.08	1.8%
H_2O−EtOH[19]	0.212	0.219	3.3%	7.86	7.978	1.5%	2.48	2.36	4.8%

[a] Uncertainty of viscosity measurements is less than 1%.

TABLE 3: Comparison between Results of D^T (10^{-12} m^2/s/K) for Binary Mixtures THN−IBB (50 wt %), THN−nC_{12} (50 wt %), IBB−nC_{12} (50 wt %), and H_2O−EtOH (60.88 wt % H_2O)[a]

mixtures	literature	our results	max Δ
THN−nC_{12}[18]	5.9 ± 0.3	5.88 ± 0.2	0.3%
THN−IBB[18]	2.8 ± 0.1	2.81 ± 0.13	0.4%
IBB−nC_{12}[18]	3.7 ± 0.2	3.85 ± 0.15	4.1%
H_2O−EtOH[19]	1.37 ± 0.1	1.34 ± 0.01	2.2%
H_2O−EtOH[20]	1.46	1.34 ± 0.01	8.3%
H_2O−EtOH[21]	1.32	1.34 ± 0.01	1.1%
H_2O−EtOH[22]	1.36	1.34 ± 0.01	1.6%
H_2O−EtOH[23]	1.31	1.34 ± 0.01	2.3%

[a] There is very good agreement between our values and literature values for all mixtures. Reference 19 measures D at 22.5 °C. All other values are at 25.0 °C. Note that the result from ref 20 for H_2O−EtOH is different from the rest.

long enough period of time, the first term ($m = 0$) in eq 8 is dominant; the expression can be then simplified to yield the following working equation

$$\frac{4L^2}{\pi^2}\ln\left(\frac{8(\omega_{1,0} - \omega_{1,\infty})}{\pi^2(\langle\omega_1\rangle - \omega_{1,\infty})}\right) = Dt \qquad (9)$$

The left-hand side of eq 9 versus time provides D for the binary mixtures. The shortcoming of this technique is that it is restricted to nonvolatile mixtures; it cannot be used for binary mixtures containing nC_5−nC_7. When available, we used literature data[5,11] for binary mixtures containing these components.

V. Results

A. Compositional and Thermal Expansion Coefficients and Calibration Curves. Figure 1a shows the density variation with composition of the MN−nC_i mixtures and the fit of eq 3 to the data. These are the calibration curves used to determine the parameters a_0 and a_1 from eq 3 and the compositional coefficient $\gamma = \rho_0^{-1}(\partial\rho/\partial\omega)$. It is clear that γ for each mixture is constant in the composition range used. Figure 1b shows the density variation with temperature around the working temperature. We obtain the thermal expansion coefficient from a linear fit to the data. All other mixtures exhibit linear dependency of density with composition and temperature. Results for all γ and α are shown in Table 1.

B. Experimental Setup Validation. Table 2 shows our results and literature values for compositional coefficient, thermal expansion coefficient, and dynamic viscosity measurements for the validation mixtures. Table 3 shows results for D^T for the validation mixtures, determined from an average of three runs. Table 4 shows D, determined in duplicate runs.

We obtained excellent agreement with literature data for molecular and thermal diffusion coefficients, dynamic viscosity, and compositional and thermal expansion coefficients for all mixtures used in the validation, expect for one data point in D. The mixture showing the largest deviation in D from the literature (THN−nC_{12}) also presents a relatively large deviation in γ; this deviation explains the discrepancy in D. With the validation results shown here, we are confident that the setups can be used to measure D and D^T reliably and accurately.

TABLE 4: Comparison between Results of D (10^{-10} m^2/s) for Binary Mixtures THN−IBB (50 wt %), THN−nC_{12} (50 wt %), IBB−nC_{12} (50 wt %), and H_2O−EtOH (60.88 wt % H_2O)[a]

		our results		
	literature values	run 1	run 2	max Δ
THN−nC_{12}[18]	6.21 ± 0.06	6.77 ± 0.10	6.77 ± 0.20	9.0%
THN−IBB[18]	8.5 ± 0.6	8.35 ± 0.33	8.77 ± 0.18	3.2%
IBB−nC_{12}[18]	9.5 ± 0.4	9.51 ± 0.57	9.47 ± 0.43	0.3%
H_2O−EtOH[19]	4.32 ± 0.26	4.15 ± 0.29	4.32 ± 0.32	3.9%
H_2O−EtOH[20]	4.15	4.15 ± 0.29	4.32 ± 0.32	4.1%
H_2O−EtOH[21]	4.19	4.15 ± 0.29	4.32 ± 0.32	3.1%
H_2O−EtOH[22]	4.19	4.15 ± 0.29	4.32 ± 0.32	3.1%

[a] The maximum deviation from literature data is less than 4.1% for all mixtures, expect for THN−nC_{12}. This mixture also exhibits a relatively large deviation on the compositional coefficient compared to literature values, which might explain the deviation in D. Reference 19 measures D at 22.5 °C. All other literature values are at 25.0 °C.

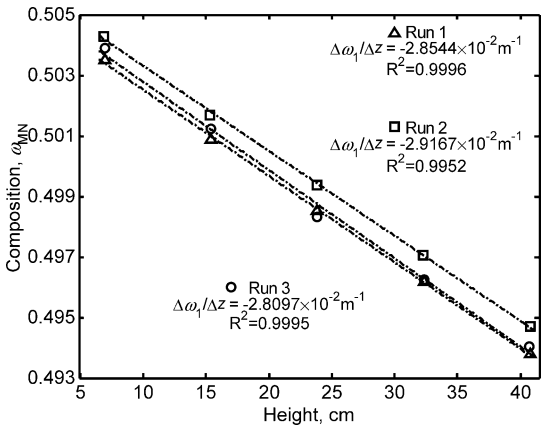

Figure 3. Composition versus height in thermogravitational column for the MN−nC_{11} binary mixture. Results are for triplicate runs. For the sake of brevity, we show only this mixture; similar results were obtained for all other binary mixtures.

C. Thermal Diffusion Coefficients. Figure 3 shows the composition variation with height in the thermogravitational column at steady state for the MN−nC_{11} mixture. We varied the temperature difference across the column between 5 and 10 °C to verify that the composition variation inside the column was independent of temperature. We performed at least triplicate runs for all mixtures and obtained results similar to Figure 3 (not shown for brevity). We calculate D^T from the average slope of all runs and determine D^T accuracy from the largest difference between the slope of each run and the average slope. The components in SET 2 have densities close to that of nC_{10}; therefore, the D^T accuracy is less than that of SET 1. Within SET 2, the more accurate measurements were those for the least volatile components and with a large enough density difference

TABLE 5: Concentration Gradient in the Column at Steady State, and Thermal Diffusion Coefficient for the Binary Mixtures at 25.0 °C and 1 atm[a]

mixture	$\Delta\omega_1/\Delta z$ (10^{-2} m^{-1})	D^T (10^{-12} m^2·s^{-1}·K^{-1})
	SET 1: MN−nC$_i$	
MN−nC$_5$	−3.12 ± 0.11	30.01 ± 1.08
MN−nC$_6$	−2.93 ± 0.02	20.89 ± 0.15
MN−nC$_7$	−2.85 ± 0.02	15.98 ± 0.10
MN−nC$_8$	−2.89 ± 0.06	12.94 ± 0.29
MN−nC$_9$	−2.83 ± 0.03	10.41 ± 0.10
MN−nC$_{10}$	−2.84 ± 0.01	8.93 ± 0.03
MN−nC$_{11}$	−2.86 ± 0.06	7.61 ± 0.15
MN−nC$_{12}$	−2.50 ± 0.04	5.67 ± 0.09
MN−nC$_{14}$	−2.71 ± 0.02	4.76 ± 0.04
MN−nC$_{16}$	−2.765 ± 0.002	3.876 ± 0.002
	SET 2: nC$_{10}$−nC$_i$	
nC$_{10}$−nC$_5$	−0.88 ± 0.02	9.64 ± 0.19
nC$_{10}$−nC$_6$	−0.88 ± 0.02	7.79 ± 0.21
nC$_{10}$−nC$_7$	−0.83 ± 0.08	5.99 ± 0.56
nC$_{10}$−nC$_8$	−0.63 ± 0.02	3.86 ± 0.14
nC$_{10}$−nC$_{12}$	0.52 ± 0.12	−1.85 ± 0.41
nC$_{10}$−nC$_{14}$	0.93 ± 0.08	−2.65 ± 0.22
nC$_{10}$−nC$_{16}$	1.42 ± 0.04	−3.35 ± 0.09
nC$_{10}$−nC$_{20}$	1.34 ± 0.02	−2.31 ± 0.04

[a] $\Delta\omega_1/\Delta z$ and D^T shown are for MN in SET 1 (MN−nC$_i$) and for nC$_{10}$ in SET 2 (nC$_{10}$−nC$_i$).

TABLE 6: Molecular Diffusion Coefficient for SET 1 (MN−nC$_i$) and SET 2 (nC$_{10}$−nC$_i$) at 25.0 °C and Atmospheric Pressure (50 wt % of each component)[a]

mixture	D (10^{-9} m^2·s^{-1})
SET 1: MN−nC$_i$	
MN−nC$_8$	1.26 ± 0.05
MN−nC$_9$	0.87 ± 0.03
MN−nC$_{10}$	0.71 ± 0.02
MN−nC$_{11}$	0.59 ± 0.02
MN−nC$_{12}$	0.46 ± 0.01
MN−nC$_{14}$	0.38 ± 0.02
MN−nC$_{16}$	0.31 ± 0.01
SET 2: nC$_{10}$−nC$_i$	
nC$_{10}$−nC$_5$[11]	2.50 ± 0.20
nC$_{10}$−nC$_7$[5]	2.23 ± 0.11
nC$_{10}$−nC$_8$	1.84 ± 0.18
nC$_{10}$−nC$_{12}$	1.18 ± 0.12
nC$_{10}$−nC$_{14}$	0.90 ± 0.07
nC$_{10}$−nC$_{16}$	0.68 ± 0.06
nC$_{10}$−nC$_{20}$	0.47 ± 0.01

[a] The error was based on the coefficient of correlation (R^2) of each linear fit.

(nC$_{16}$ and nC$_{20}$). Because of close densities between the components, we did not measure the D^T for mixtures nC$_9$−nC$_{10}$ and nC$_{11}$−nC$_{10}$. In SET 1, D^T of MN is positive for all mixtures: MN behaves as the thermophobic species, segregating to the cold side and bottom of the column. In SET 2, nC$_{10}$ segregates to the cold side and bottom of the column for mixtures with nC$_i$ < nC$_{10}$ (behaving thermophobically); for nC$_i$ > nC$_{10}$, it behaves as the thermophilic species, segregating to the hot side and top of the column. Therefore, nC$_{10}$ for SET 2 displays a sign change in D^T. Table 5 shows the composition slopes along the column and D^T for all mixtures.

D. Molecular Diffusion Coefficients. Figure 4a shows a plot of the left-hand side of eq 9 versus time for SET 1; Figure 4b shows a similar plot for SET 2. For a given binary mixture, D is the slope of its respective curve; all results are shown in Table 6. The binary mixtures that contain highly volatile components (nC$_5$− nC$_7$) cannot be determined using the open-ended capillary tube technique. We found data in the literature for mixtures nC$_5$−nC$_{10}$ and nC$_7$−nC$_{10}$ at atmospheric pressure and temperature close to 25 °C but different compositions.[5,11] We estimated D values for these mixtures at $\omega = 0.5$ by second-degree polynomial interpolation (also shown in Table 6). The accuracy of the D measurements was estimated from the coefficient of correlation (R^2) of each fit. We observe more scatter in Figure 4b (SET 2) than in Figure 4a (SET 1) since the density difference between the mixture components is smaller for SET 2 than for SET 1. The scatter is reflected in the measurement accuracy.

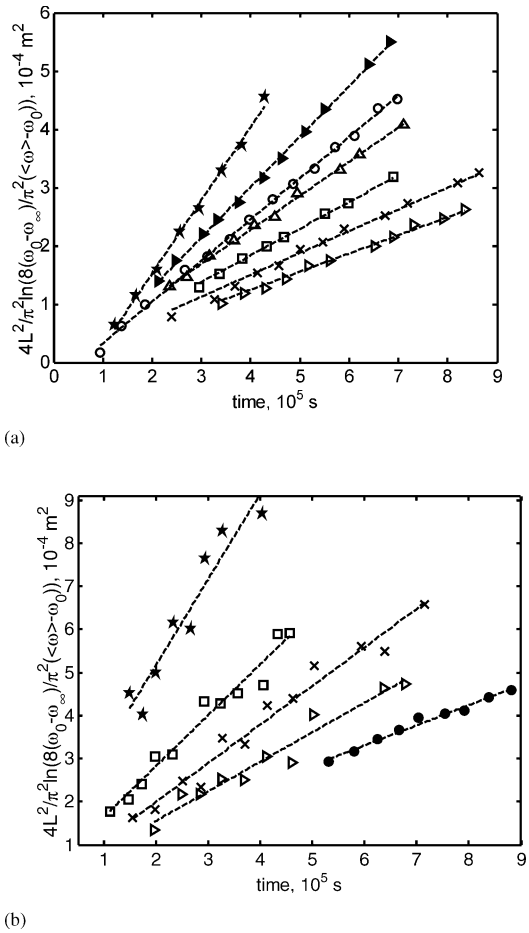

Figure 4. Left-hand side of eq 9 versus time for binary mixtures MN−nC$_8$ (★), MN−nC$_9$ (solid right-facing triangle), MN−nC$_{10}$ (○), MN−nC$_{11}$ (△), MN−nC$_{12}$ (□), MN−nC$_{14}$ (×), and MN−nC$_{16}$ (open right-facing triangle) (Figure a) and for binary mixtures nC$_{10}$−nC$_8$ (★), nC$_{10}$−nC$_{12}$ (□), nC$_{10}$−nC$_{14}$ (×), nC$_{10}$−nC$_{16}$ (open right-facing triangle), and nC$_{10}$−nC$_{20}$ (●) (Figure b). All measurements are at 50 wt % of each component, 25.0 °C, and 1 atm. The slope of the dashed lines is D for each mixture.

VI. Discussion

A. Effect of Molecular Shape. Figure 5 depicts the essence of our thermal diffusion coefficients D^T for the two sets, where the data are plotted versus the respective normalized alkane molecular weight (the ratio of normal alkane molecular weight to either nC$_{10}$ or MN molecular weight). The thermal diffusion coefficients are generally greater for SET 1 (MN−nC$_i$) than for SET 2 (nC$_{10}$−nC$_i$) up to the normalized molecular weight of about 1.4. Normal alkanes have similar molecular configuration and therefore respond similarly to a temperature gradient, which explains the small D^T values in SET 2. On the other hand, MN has a very different molecular structure and shape compared to normal alkanes, which results in large D^Ts for SET 1 (up to the normalized molecular weight of 1.4). Figure 5 also shows

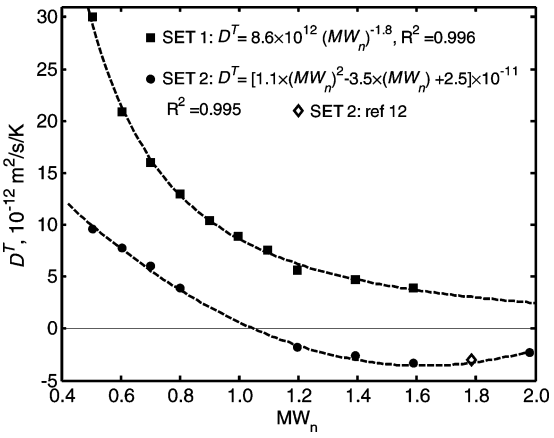

Figure 5. Thermal diffusion coefficients versus normalized molecular weight of normal alkanes for SET 1 (MN−nC$_i$) and SET 2 (nC$_{10}$−nC$_i$), with 50 wt % each component, at 25 °C and 1 atm. The dashed lines represent fits to the data. MW$_n$ is the molecular weight of the alkane molecule, normalized by the molecular weight of MN (SET 1) or nC$_{10}$ (SET 2). The D^T shown is for MN in SET 1 and for nC$_{10}$ for SET 2.

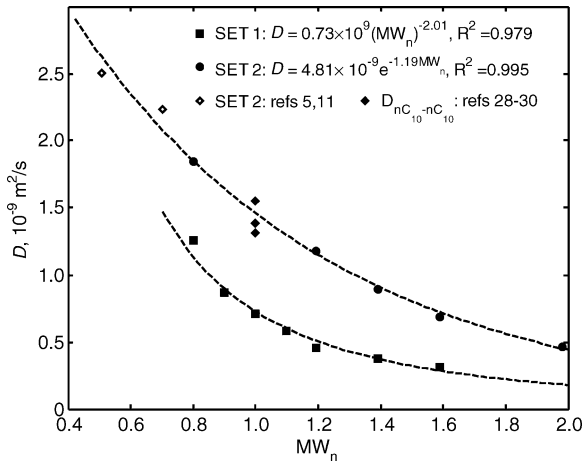

Figure 6. Molecular diffusion coefficient versus normalized molecular weight of normal alkanes (MW$_n$) for SET 1 (MN−nC$_i$) and SET 2 (nC$_{10}$−nC$_i$) at 50 wt % each component, 25 °C, and 1 atm. Values of D for nC$_{10}$−nC$_5$ and nC$_{10}$−nC$_7$ are from refs 11 and 5, respectively.

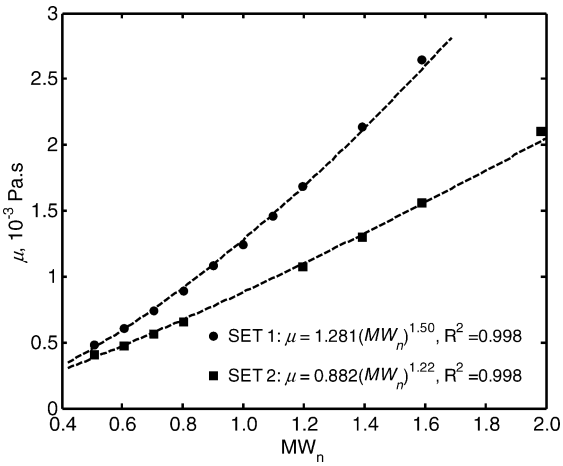

Figure 7. Mixture dynamic viscosity versus normalized alkane molecular weight (MW$_n$) for SET 1 (MN−nC$_i$) and SET 2 (nC10−nC$_i$) at 50 wt % each component, 25 °C, and 1 atm. The dashed lines represent power fits to the data.

the best fits to both data sets along with respective coefficients of correlation (R^2). A power fit describes SET 1 very well, while it fails to represent SET 2. We expect that for SET 1 D^T will continue to decrease smoothly as the molecular weight of the alkane increases until it reaches a positive asymptotic value. We expect a similar trend for other aromatic−normal alkane mixtures, provided the aromatic does not contain functional groups that change its chemical activity, such as nitrile, hydroxyl, or halide groups among others. In fact, Polyakov et al.[14] recently measured D^T and D for equimolar mixtures of benzene−nC$_i$ (i = 7, 9, 11, 13, 15) at 20 °C. They observed a trend in their D^T data very similar to that of SET 1.

The behavior of D^T in SET 2 is very different. Exponential, logarithmic, and power law fits fail to represent SET 2. Within the range studied it is best represented by a second-degree polynomial fit, although it cannot be used to estimate D^T outside the range. For this set, D^T becomes zero at nC$_i$ = nC$_{10}$ as expected, reaches a minimum (negative) around nC$_i$ = nC$_{16}$, and decreases in magnitude for heavier alkane molecules; we expect it to reach a small negative asymptotic value for large alkane molecular weights. In the MN−nC$_i$ set the trend is monotonic, while in the nC$_{10}$−nC$_i$ set there is nonmonotonic behavior when results are plotted versus the normalized molecular weight. Blanco et al.[12] measured D^T for nC$_{10}$−nC$_{18}$ at 50 wt % each component and 25 °C. Our predicted value for nC$_{10}$−nC$_{18}$ fits very well to their data and confirms the nonmonotonic behavior of SET 2. These results suggest that molecular shape is important in thermal diffusion coefficients.

The effect of molecular shape on molecular diffusion coefficient D also becomes evident when analyzing Figure 6; SETs 1 and 2 show different behaviors. SET 1 is best described by a power law, while SET 2 is best represented by an exponential fit. Again, a trend very similar to that of SET 1 is observed in the benzene−alkane system.[14] For SET 2 we can obtain the self-molecular diffusion coefficient of nC$_{10}$ from the best fit of the data. The predicted value of $D_{nC_{10}-nC_{10}} = 1.46 \times 10^{-9}$ m^2/s from Figure 6 is in agreement with literature data[28−30] despite the fact that there is noticeable scatter in measurements from refs 28−30.

There have been a few attempts in the literature[4,31−33] to correlate molecular diffusion coefficients to mixture viscosity or solvent viscosity (for dilute systems). For our mixtures Figure 7 shows that mixture dynamic viscosity is a function of alkane molecular weight, since the alkanes used are part of the same homologous series. The same behavior for the data in Figures 5 and 6 is observed when plotting diffusion coefficients against mixture dynamic viscosity (plots are not shown for the sake of brevity). However, the plot of D^T for SET 1 shows a nonmonotonic trend which has not been reported in the literature.

B. Effect of n-Alkane Chain Length. When relating diffusion data to the alkane chain length we hypothesize that there are two opposing factors that affect the diffusion coefficients, which we call the *mobility* of each individual component and the *similarity* between the components.

The *mobility* of each component is associated to Brownian motion of molecules; at a given temperature it is a function of self-molecular diffusion coefficient and viscosity.[34−36] Increasing self-molecular diffusion coefficients and decreasing viscosity contribute to an increase in mobility. Kramers and Broeder[37] related component mobility to thermal diffusion in liquid mixtures. In the case of normal alkanes, the heavier the molecule, the less mobile it is (for normal alkanes self-molecular diffusion coefficient decreases with increasing molecular weight).[38] The *similarity* between the components relates to how differently each component will respond to a given force field. Physical properties such as boiling point, heat capacity, latent heat of

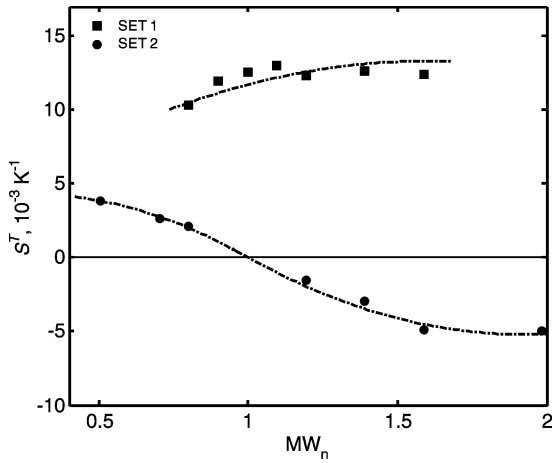

Figure 8. Soret coefficient (D^T/D) versus normalized molecular weight of alkanes (MW_n) for SET 1 (MN−nC_i) and SET 2 (nC_{10}−nC_i). Dashed lines represent fits to the data for each set; S^T shown is for MN (SET 1) and nC_{10} (SET 2).

vaporization, and critical properties may relate to *similarity* between components. These properties are related not only to the shape and size of molecules but also to the molecular interactions.

For thermal diffusion, similarity between components decreases D^T: alike molecules respond very similarly to temperature gradients and hardly separate. Component mobility increases D^T: more mobile molecules respond more strongly to a temperature gradient field.

To illustrate the above idea we examine SET 2 in Figure 5. From nC_5 to nC_{10}, increasing the molecular weight of the normal alkane decreases nC_i mobility and increases similarity between nC_i and nC_{10}; both factors decrease D^T. As $nC_i = nC_{10}$ (where similarity is maximum), similarity changes behavior and now decreases while mobility keeps decreasing. In this case the two factors have competing effects; until $nC_i = nC_{16}$ the similarity factor has a more important effect: D^T increases in magnitude since the molecules are becoming less similar, even though they are also becoming less mobile. For $nC_i > nC_{16}$, the mobility factor dominates and D^T decreases in magnitude, even though the molecules become less similar. This effect will dominate thermal diffusion for this set for all normal alkanes larger than nC_{16}.

For SET 1 both effects are also present. Mobility decreases as alkane molecular weight decreases; however, we cannot determine at this point how the similarity factor between nC_i and MN changes; it seems to be increasing with increasing alkane molecular weight, therefore acting concurrently with mobility and decreasing D^T.

Figure 6 shows that molecular diffusion coefficients D in SET 2 are greater than those in SET 1. Analysis of benzene−alkane data[14] shows that D for all benzene−nC_i mixtures is greater than that for SET 1 and SET 2, even though nC_i molecules are more similar to nC_{10} than to MN and benzene. This indicates that the mobility factor dominates molecular diffusion and the similarity factor is negligible. When we compare the self-molecular diffusion coefficient and viscosities of nC_{10}, benzene, and MN at temperatures at or around 25 °C, we find that $D_{benz-benz}$[39] > $D_{nC10-nC10}$[30] > D_{MN-MN},[40] and μ_{benz}[41] < μ_{nC10} < μ_{MN};[42] among the three, benzene is the most mobile molecule, followed by nC_{10} and then MN. According to the mobility factor, D for the benzene−alkane mixtures should be greater than D for SET 2, followed by D for SET 1. This is what we observe experimentally.

As a final remark, we study the ratio of molecular to thermal diffusion coefficients, generally referred to as the Soret coefficient, $S^T = (D^T/D)$. We plot S^T for both sets in Figure 8. The Soret coefficient is less accurate than both D^T and D since the bounds of the relative errors in both coefficients are added.[43] For SET 1, S^T increases slowly with normalized molecular weight of the alkanes. For SET 2, S^T decreases with normalized alkane molecular weight, passing through zero at $nC_i = nC_{10}$. There is an inflection point at $nC_i = nC_{10}$, where the curvature changes sign, reflecting the different behaviors of S^T for $nC_i > nC_{10}$ and $nC_i < nC_{10}$.

We also comment on the complexity of using S^T in place of D and D^T for ternary and higher mixtures as the Soret coefficient concept lacks generality. For multicomponent mixtures with n components, there are $(n-1)$ D^T, $(n/2)(n-1)$ independent D, and many different ways the ratio between such coefficients can be defined.

VII. Conclusions

In this work we provide a systematic set of new measurements for two drastically different sets of binary hydrocarbon mixtures. In one set, comprised of binary mixtures of nC_{10} and normal alkanes (nC_5−nC_{20}), molecular and thermal diffusion coefficients show a different trend when plotted versus the normal alkane molecular weight. Thermal diffusion coefficients reveal a nonmonotonic trend which may be due to the competing effect of molecular mobility and similarity. In another set, comprised of binary mixtures of 1-methylnaphthalene and normal alkanes (nC_5−nC_{16}), the thermal and molecular diffusion coefficient data show a significant effect of molecular shape.

Interestingly, the plot of thermal diffusion coefficient data versus alkane molecular weight for the nC_{10}−normal alkane set provides a value of $D^T \approx 0$ for pure nC_{10}. A similar plot for the nC_{10}−normal alkane molecular diffusion coefficient provides the self-molecular diffusion coefficient of nC_{10}; the value is in agreement with the measured literature value.

Acknowledgment. This work was supported by the member companies of the Reservoir Engineering Research Institute (RERI) in Palo Alto, CA.

References and Notes

(1) Ghorayeb, K.; Firoozabadi, A. *AIChE J.* **2000**, *46*, 883.
(2) Firoozabadi, A; Ghorayeb, K.; Shukla, K. *AIChE J.* **2000**, *46*, 892.
(3) Kempers, L. J. T. M. *J. Chem. Phys.* **1989**, *90*, 6541.
(4) Hayduck, W.; Buckley, W. D. *Chem. Eng. Sci.* **1972**, *27*, 1997.
(5) Lo, H. Y. *J. Chem. Eng. Data* **1974**, *19*, 236.
(6) Rowley, R. L.; Yi, S. C.; Gubler, V.; Stoker, J. M. *Fluid Phase Equilib.* **1987**, *36*, 219.
(7) Rowley, R. L.; Yi, S. C.; Gubler, V.; Stoker, J. M. *J. Chem. Eng. Data* **1988**, *33*, 362.
(8) Shieh, J. J. C. *J. Phys. Chem.* **1969**, *73*, 1508.
(9) Debuschewitz, C; Köhler, W. *Phys. Rev. Lett.* **2001**, *87*, 055901.
(10) Wittko, G.; Köhler, W. *J. Chem. Phys.* **2005**, *123*, 014506.
(11) Perronace, A.; Leppla, C.; Leroy, F.; Rousseau, B.; Wiegand, S. *J. Chem. Phys.* **2002**, *116*, 3718.
(12) Blanco, P.; Bou-Ali, M. M.; Platten, J. K.; Madariaga, J. A.; Urteaga, P.; Santamaría, C. In *Thermodiffusion: Basics & Application*; Bou-Ali, M. M., Platten, J. K., Eds.; San Sebastian, Spain, 2006; pp 427−438.
(13) Demichowicz-Pigoniowa, J.; Mitchell, M.; Tyrrell, H. J. V. *J. Chem. Soc. (A)* **1971**, *2*, 307.
(14) Polyakov, P.; Wiegand, S. In *Thermodiffusion: Basics & Application*; Bou-Ali, M. M., Platten, J. K., Eds.; San Sebastian, Spain, 2006; pp 399−407.
(15) Bou-Ali, M. M. Ph.D. Thesis, Universidad del Pais Vasco, Spain, 1999.
(16) Zhang, K. J.; Briggs, M. E.; Gammon, R. W.; Sengers, J. V. *J. Chem. Phys.* **1996**, *104*, 6881.
(17) Leahy-Dios, A.; Bou-Ali, M. M.; Platten, J. K.; Firoozabadi, A. *J. Chem. Phys.* **2005**, *122*, 234502.

(18) Platten, J. K.; Bou-Ali, M. M.; Costèsèque, P.; Dutrieux, J. F.; Köhler, W.; Leppla, C.; Wiegand, S.; Wittko, G. *Philos. Mag.* **2003**, *83*, 1965.
(19) Dutrieux, J. F.; Platten, J. K.; Chavepeyer, G.; Bou-Ali, M. M. *J. Phys. Chem. B* **2002**, *106*, 6104.
(20) Zhang, K. J.; Briggs, M. E.; Gammon, R. W.; Sengers, J. V. *J. Chem. Phys.* **1996**, *104*, 6881.
(21) Kolodner, P.; Williams, H.; Moe, C. *J. Chem. Phys.* **1988**, *88*, 6512.
(22) Köhler, W.; Müller, B. *J. Chem. Phys.* **1995**, *103*, 4367.
(23) Bou-Ali, M. M.; Ecenarro, O.; Madariaga, J. A.; Santamaria, C. M.; Valencia, J. J. *Entropie* **1999**, *5*, 218.
(24) Furry, W. H.; Jones, R. C.; Onsager, L. *Phys. Rev.* **1939**, *55*, 1083.
(25) Majumdar, S. D. *Phys. Rev.* **1951**, *81*, 844.
(26) Haugen, K. B.; Firoozabadi, A. *J. Chem. Phys.* **2005**, *122*, 014516.
(27) Cussler, E. L. *Diffusion: Mass Transfer in Fluid Systems*; Cambridge University Press: Cambridge, 1997.
(28) Douglass, D. C.; McCall, D. W. *J. Phys. Chem.* **1958**, *62*, 1102.
(29) Moore, J. W.; Wellek, R. M. *J. Chem. Eng. Data* **1974**, *19*, 136.
(30) Tofts, P. S.; Lloyd, D.; Clark, C. A.; Baker, G. J.; Parker, G. J. M.; McConville, P.; Baldock, C.; Pope, J. M. *Magn. Reson. Med.* **2000**, *3*, 368.
(31) Hayduck, W.; Ioakimidis, S. *J. Chem. Eng. Data* **1976**, *21*, 255.
(32) Leffer, J.; Cullinan, H. T. *Ind. Eng. Chem.* **1970**, *9*, 84.
(33) Dullien, F. A. L.; Asfour, A.-F. A. *Ind. Eng. Chem. Fundam.* **1985**, *24*, 1.
(34) Tyrrell, H. J. V.; Harris, K. R. *Diffusion in Liquids: A theoretical and experimental study*; Cambridge University Press: London, 1984.
(35) Groot, S. R.; Mazur, P. *Non-equilibrium thermodynamics*; Dover Publications: Mineola, 1984.
(36) Reif, F. *Fundamentals of statistical and thermal physics*; McGraw-Hill: New York, 1965.
(37) Kramers, H.; Broeder, J. J. *Anal. Chim. Acta* **1948**, *2*, 687.
(38) Van Geet, A. L.; Adamson, A. W. *Ind. Eng. Chem.* **1965**, *57*, 62.
(39) Caldwell, C. S.; Babb, A. L. *J. Phys. Chem.* **1956**, *60*, 51.
(40) D_{MN-MN} estimated from the Stokes−Einstein equation.
(41) Geist, J. M.; Cannon, M. R. *Ind. Eng. Chem. Anal. Ed.* **1946**, *18*, 611.
(42) Yaws, C. L. *Handbook of Viscosity*; Gulf Publishing Co.: Houston, 1995; Vol. 3.
(43) Dahlquist, G.; Bjorck, A. *Numerical Methods*; Dover Publications: New York, 2003.